

Helicity Evolution at Small x : Summary of Recent Developments

Yuri V. Kovchegov

*Department of Physics, The Ohio State University, Columbus, OH 43210, USA**

Daniel Pitonyak

Division of Science, Penn State University-Berks, Reading, PA 19610, USA†

Matthew D. Sievert

Theoretical Division, Los Alamos National Laboratory, Los Alamos, NM 87545, USA‡

(Dated: November 12, 2021)

We construct small- x evolution equations which can be used to calculate quark and anti-quark helicity TMDs and PDFs, along with the g_1 structure function. These evolution equations resum powers of $\alpha_s \ln^2(1/x)$ in the polarization-dependent evolution along with the powers of $\alpha_s \ln(1/x)$ in the unpolarized evolution which includes saturation effects. The equations are written in an operator form in terms of polarization-dependent Wilson line-like operators. While the equations do not close in general, they become closed and self-contained systems of non-linear equations in the large- N_c and large- N_c & N_f limits. We construct a numerical solution of the helicity evolution equations in the large- N_c limit. Employing the extracted intercept, we are able to predict directly from theory the behavior of the quark helicity PDFs at small x , which should have important phenomenological consequences. We also give an estimate of how much of the proton's spin may be at small x and what impact this has on the so-called "spin crisis."

I. INTRODUCTION

These proceedings are based on the work done in [1–3].

Our aim is to derive perturbative QCD prediction for the asymptotic small Bjorken x behavior of the quark and gluon helicity distribution functions and for related observables. In these proceedings we will concentrate on the flavor-singlet quark helicity distribution $\Delta q(x, Q^2)$. We will derive helicity evolution equations resumming powers of $\alpha_s \ln^2(1/x)$ with α_s the strong coupling constant: this resummation is referred to as the double-logarithmic approximation (DLA). These evolution equations allow one to determine the leading perturbative behavior of the small- x asymptotics of $\Delta q(x, Q^2)$ (see [2, 3]). Such theoretical input is necessary to assist the efforts to determine the small- x part of the quark contribution to proton spin

$$S_q(Q^2) = \frac{1}{2} \int_0^1 dx \Delta \Sigma(x, Q^2),$$

$$\Delta \Sigma(x, Q^2) = [\Delta u + \Delta \bar{u} + \Delta d + \Delta \bar{d} + \dots](x, Q^2), \quad (1)$$

where the helicity parton distribution functions (hPDFs) are

$$\Delta f(x, Q^2) \equiv f^+(x, Q^2) - f^-(x, Q^2). \quad (2)$$

The ultimate goal of determining the proton spin carried by quarks [and the spin carried by the gluons, $S_G(Q^2)$] is to resolve the proton spin crisis.

II. THE OBSERVABLES

The small- x helicity observables can be obtained by studying the cross section for semi-inclusive deep inelastic scattering (SIDIS) on a longitudinally polarized target, $\gamma^* + \vec{p} \rightarrow \vec{q} + X$. The contributions are shown diagrammatically in Fig. 1 (see [4] for a derivation).

The corresponding flavor-singlet quark helicity transverse momentum-dependent parton distribution function (TMD) is [1]

$$g_{1L}^S(x, k_T^2) = \frac{8 N_c}{(2\pi)^6} \sum_f \int_{z_i}^1 \frac{dz}{z} \int d^2 x_\perp d^2 y_\perp e^{-ik \cdot (x-y)} \times \frac{\underline{x} - \underline{w}}{|\underline{x} - \underline{w}|^2} \cdot \frac{\underline{y} - \underline{w}}{|\underline{y} - \underline{w}|^2} d^2 w_\perp G_{\underline{x}, \underline{w}}(z). \quad (3)$$

The notation is explained in Fig. 1. Here $\underline{k} = (k^x, k^y)$ denotes transverse vectors, with $k_\perp = |\underline{k}|$. Variable z denotes the fraction of the virtual photon's longitudinal momentum carried by the anti-quark with $z_i = \Lambda^2/s$, where Λ is the infra-red (IR) cutoff, and s is the SIDIS center-of-mass energy squared. The object G is the *polarized dipole amplitude*, which is defined by [1]

$$G_{10}(z) \equiv \frac{1}{2N_c} \left\langle \left\langle \text{tr} [V_0 V_1^{pol\dagger}] + \text{tr} [V_1^{pol} V_0^\dagger] \right\rangle \right\rangle(z), \quad (4a)$$

$$G(x_{01}^2, z) \equiv \int d^2 b G_{10}(z), \quad (4b)$$

where $\underline{b} = (1/2)(\underline{x}_1 + \underline{x}_0)$. The propagator of an eikonal quark with polarization σ in the background quark or gluon field of the target proton is written as

$$V_{\underline{x}}(\sigma) \equiv V_{\underline{x}} + \sigma V_{\underline{x}}^{pol} \quad (5)$$

* Email: kovchegov.1@osu.edu

† Email: dap67@psu.edu

‡ Email: sievertmd@lanl.gov

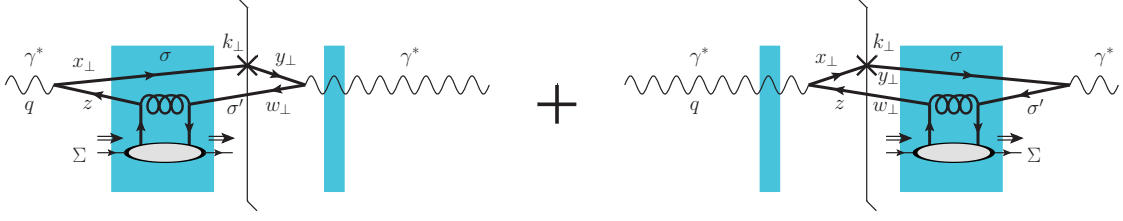


FIG. 1. Diagrams contributing to the small- x SIDIS process on a longitudinally polarized target, and to quark helicity TMD $g_{1L}^q(x, k_T)$.

where

$$V_{\underline{x}} \equiv \text{P exp} \left[ig \int_{-\infty}^{\infty} dx^+ A^-(x^+, 0^-, \underline{x}) \right] \quad (6)$$

is the light-cone Wilson line, and V^{pol} is the helicity-dependent sub-eikonal correction. The double angle brackets indicate averaging in the target wave function, with an inverse factor of center-of-mass energy squared scaled out:

$$\langle \dots \rangle (z) = \frac{1}{z s} \langle \langle \dots \rangle \rangle (z). \quad (7)$$

The polarized dipole amplitude can be used to obtain other helicity observables. The flavor-singlet quark helicity PDF,

$$\Delta q^S(x, Q^2) \equiv \sum_f [\Delta q^f(x, Q^2) + \Delta \bar{q}^f(x, Q^2)], \quad (8)$$

at small- x is equal to

$$\Delta q^S(x, Q^2) = \frac{N_c}{2\pi^3} \sum_f \int_{z_i}^1 \frac{dz}{z} \int \frac{d^2\underline{x}}{|\underline{x} - \underline{w}|^2} G(|\underline{x} - \underline{w}|^2, z). \quad (9)$$

The g_1 structure function is

$$g_1^S(x, Q^2) = \frac{N_c}{2\pi^2 \alpha_{EM}} \sum_f \int_{z_i}^1 \frac{dz}{z^2(1-z)} \int d^2\underline{x} - \underline{w}^2 \times \left[\frac{1}{2} \sum_{\lambda\sigma\sigma'} |\psi_{\lambda\sigma\sigma'}^T|^2_{(|\underline{x} - \underline{w}|^2, z)} + \sum_{\sigma\sigma'} |\psi_{\sigma\sigma'}^L|^2_{(|\underline{x} - \underline{w}|^2, z)} \right] \times G(|\underline{x} - \underline{w}|^2, z), \quad (10)$$

where ψ^T and ψ^L are the well-known light cone wave functions for the $\gamma^* \rightarrow q\bar{q}$ splitting (see e.g. [1]).

Our aim is to find the small- x evolution equations for the polarized dipole amplitude $G_{10}(z)$. Once $G_{10}(z)$ is found, we can use Eqs. (3), (9) and (10) to construct the flavor-singlet quark helicity TMD, PDF and the g_1 structure function.

III. LARGE- N_c LIMIT

Similar to the case of JIMWLK evolution and Balitsky hierarchy, the general evolution equation for $G_{10}(z)$ does not close: on its right-hand side it contains operator expectation values other than $G_{10}(z)$. The operators on the right-hand side contain higher number of Wilson lines than $G_{10}(z)$. This leads to the helicity evolution analogue of the Balitsky hierarchy.

However, also similar to the unpolarized (BK) case, the evolution equations become closed equations involving $G_{10}(z)$ in the large- N_c limit. In addition, specific to the helicity evolution case at hand, evolution equations also close in the large- N_c & N_f limit. Below we will first discuss the large- N_c case.

Here we simply quote the results, referring the reader to the derivation details in [1, 3]. Similar to [5], our evolution equations also resum the leading-logarithmic (LLA) powers of $\alpha_s \ln(1/x)$ by including the BK/JIMWLK evolved unpolarized dipole S -matrix

$$S_{01}(z) = \frac{1}{2N_c} \langle \langle \text{tr} [V_{\underline{0}} V_{\underline{1}}^\dagger] + \text{tr} [V_{\underline{1}} V_{\underline{0}}^\dagger] \rangle \rangle (z) \approx \frac{1}{N_c} \langle \langle \text{tr} [V_{\underline{0}} V_{\underline{1}}^\dagger] \rangle \rangle (z), \quad (11)$$

where we assume that

$$\text{tr} [V_{\underline{0}} V_{\underline{1}}^\dagger] = \text{tr} [V_{\underline{1}} V_{\underline{0}}^\dagger], \quad (12)$$

which is true at LLA. Note that LLA terms of the pure helicity evolution are not systematically included in this approach: hence we do not have a complete LLA calculation, and our results are strictly correct only in the DLA limit where $S_{01}(z) = 1$.

The evolution equation for $G_{10}(z)$ is illustrated in the top line of Fig. 2. Note that the large- N_c limit is gluon-dominated: hence the dipole 10 is made out of quark and anti-quark lines of the large- N_c gluon. The equation reads $(x_{ij} = |\underline{x}_i - \underline{x}_j|, \rho'^2 = 1/(z' s))$

$$G_{10}(z) = G_{10}^{(0)}(z) + \frac{\alpha_s N_c}{2\pi} \int_{1/(s x_{10}^2)}^z \frac{dz'}{z'} \int_{\rho'^2}^{x_{10}^2} \frac{dx_{21}^2}{x_{21}^2} \times [2\Gamma_{02,21}(z') S_{21}(z') + 2G_{21}(z') S_{02}(z') + G_{12}(z') S_{02}(z') - \Gamma_{01,21}(z')], \quad (13)$$

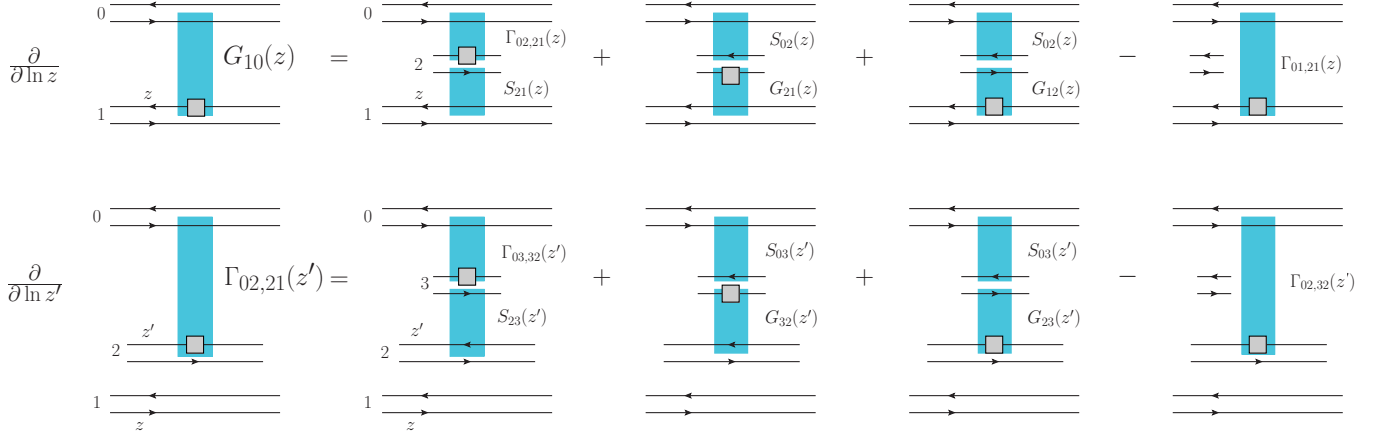


FIG. 2. Large- N_c helicity evolution for the polarized dipole amplitude G and the neighbor dipole amplitude Γ . For pictorial simplicity we do not show the contributions of the initial condition terms. Double lines denote gluons at large N_c . Only one of the virtual diagrams is shown (last diagram in each line): virtual corrections to the right of the shock wave are implied, but not shown explicitly.

where $\Gamma_{02,21}(z')$ is the new object (as compared to the unpolarized evolution), characteristic of helicity evolution. $\Gamma_{02,21}(z')$ is the “neighbor dipole” amplitude. Its evolution is described in the bottom line of Fig. 2. As shown in the figure, the “neighbor” dipole evolution continues in dipole 02, but the information about the dipole 21 comes in through the transverse size integration limit. (This is in contrast to unpolarized evolution, where the evolution in, say, dipole 02 does not depend on the size of the dipole 21 or on anything else outside the dipole 02.) The evolution for the neighbor dipole amplitude reads ($\rho''^2 = 1/(z'' s)$)

$$\Gamma_{02,21}(z') = \Gamma_{02,21}^{(0)}(z') + \frac{\alpha_s N_c}{2\pi} \int_{1/(s x_{10}^2)}^{z'} \frac{dz''}{z''} \quad (14)$$

$$\times \int_{\rho''^2}^{\min\{x_{10}^2, x_{21}^2 z'/z''\}} \frac{dx_{32}^2}{x_{32}^2} [2\Gamma_{02,32}(z'') S_{23}(z'')$$

$$+ 2G_{32}(z'') S_{03}(z'') + G_{23}(z'') S_{03}(z'') - \Gamma_{02,32}(z'')].$$

Eqs. (13) and (14), when augmented by the BK evolution for S , present a closed system of equations. The initial conditions $G^{(0)}$ and $\Gamma^{(0)}$ are given by the Born-level interactions, enhanced by multiple rescatterings which bring in saturation effects.

In the strict DLA limit we can simplify Eqs. (13) and (14) by putting $S = 1$ and assuming that $G_{21} = G_{12}$. We

obtain

$$G_{01}(z) = G_{01}^{(0)}(z) + \frac{\alpha_s N_c}{2\pi} \int_{1/(s x_{10}^2)}^z \frac{dz'}{z'} \quad (15a)$$

$$\times \int_{\rho'^2}^{x_{10}^2} \frac{dx_{21}^2}{x_{21}^2} [\Gamma_{02,21}(z') + 3G_{21}(z')],$$

$$\Gamma_{02,21}(z') = \Gamma_{02,21}^{(0)}(z') + \frac{\alpha_s N_c}{2\pi} \int_{1/(s x_{10}^2)}^{z'} \frac{dz''}{z''} \quad (15b)$$

$$\times \int_{\rho''^2}^{\min\{x_{02}^2, x_{21}^2 z'/z''\}} \frac{dx_{32}^2}{x_{32}^2} [\Gamma_{02,32}(z'') + 3G_{23}(z'')].$$

IV. LARGE- N_c & N_f LIMIT

Helicity evolution equations also close in the large- N_c & N_f limit. To write down these new evolution equations we need to define a couple of new objects. In addition to $G_{10}(z)$ defined in Eq. (4a) above, which is made out of quark and anti-quark lines of gluons (with x_1 line polarized), let us define

$$A_{10}(z) = \frac{1}{2N_c} \left\langle \left\langle \text{tr} [V_{\underline{0}} V_{\underline{1}}^{pol \dagger}] + \text{tr} [V_{\underline{1}}^{pol} V_{\underline{0}}^\dagger] \right\rangle \right\rangle(z) \quad (16)$$

with x_1 being a true quark or anti-quark polarized line and x_0 being the (anti-)quark line of the gluon, and

$$Q_{10}(z) = \frac{1}{2N_c} \left\langle \left\langle \text{tr} [V_{\underline{0}} V_{\underline{1}}^{pol \dagger}] + \text{tr} [V_{\underline{1}}^{pol} V_{\underline{0}}^\dagger] \right\rangle \right\rangle(z) \quad (17)$$

with both x_0 and x_1 being true quark and anti-quark lines and x_1 polarized.

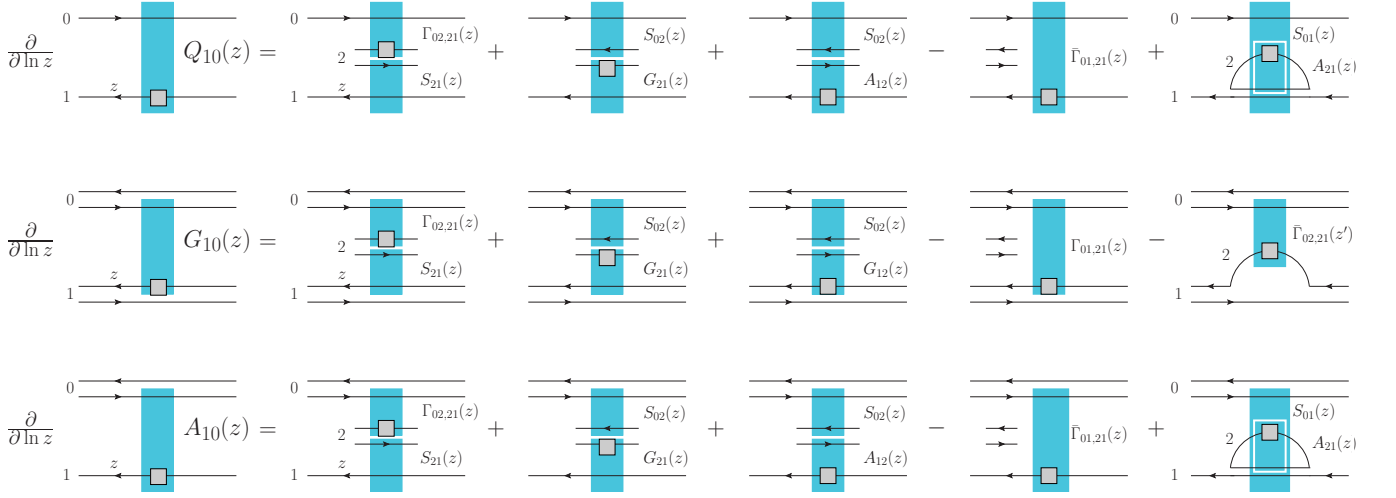


FIG. 3. Large- N_c & N_f helicity evolution for the polarized dipole amplitudes Q , G and A .

Large- N_c & N_f evolution equations for Q , G and A are illustrated diagrammatically in Fig. 3, where again we do not show the initial condition terms for simplicity. The equation for Q is

$$\begin{aligned}
Q_{10}(z) &= Q_{10}^{(0)}(z) + \frac{\alpha_s N_c}{2\pi} \int_{z_i}^z \frac{dz'}{z'} \int_{\rho'^2}^{x_{10}^2} \frac{dx_{21}^2}{x_{21}^2} \\
&\times [S_{21}(z') \Gamma_{02,21}(z') + S_{02}(z') G_{21}(z') \\
&+ S_{02}(z') A_{12}(z') - \bar{\Gamma}_{01,21}(z')] \\
&+ \frac{\alpha_s N_c}{4\pi} \int_{z_i}^z \frac{dz'}{z'} \int_{\rho'^2}^{x_{10}^2 z'/z'} \frac{dx_{21}^2}{x_{21}^2} S_{01}(z') A_{21}(z'). \quad (18)
\end{aligned}$$

Equation (18) is illustrated diagrammatically in the first line of Fig. 3. The equation for G is now

$$\begin{aligned}
G_{10}(z) &= G_{10}^{(0)}(z) + \frac{\alpha_s N_c}{2\pi} \int_{z_i}^z \frac{dz'}{z'} \int_{\rho'^2}^{x_{10}^2} \frac{dx_{21}^2}{x_{21}^2} \\
&\times [2 S_{21}(z') \Gamma_{02,21}(z') + 2 S_{02}(z') G_{21}(z') \\
&+ S_{02}(z') G_{12}(z') - \Gamma_{01,21}(z')] \\
&- \frac{\alpha_s N_f}{4\pi} \int_{z_i}^z \frac{dz'}{z'} \int_{\rho'^2}^{x_{10}^2 z'/z'} \frac{dx_{21}^2}{x_{21}^2} \bar{\Gamma}_{02,21}(z'). \quad (19)
\end{aligned}$$

Note a new object, $\bar{\Gamma}_{02,21}$, which is the neighbor dipole amplitude with line 2 being an actual polarized quark (or anti-quark), and, unlike in $\Gamma_{02,21}$, not a quark (or anti-quark) line of a large- N_c gluon. Equation (19) is illustrated diagrammatically in the second line of Fig. 3.

Finally, the evolution for $A_{01}(z)$ reads

$$\begin{aligned}
A_{10}(z) &= A_{10}^{(0)}(z) + \frac{\alpha_s N_c}{2\pi} \int_{z_i}^z \frac{dz'}{z'} \int_{\rho'^2}^{x_{10}^2} \frac{dx_{21}^2}{x_{21}^2} \\
&\times [S_{21}(z') \Gamma_{02,21}(z') + S_{02}(z') G_{21}(z') \\
&+ S_{02}(z') A_{12}(z') - \bar{\Gamma}_{01,21}(z')] \\
&+ \frac{\alpha_s N_c}{4\pi} \int_{z_i}^z \frac{dz'}{z'} \int_{\rho'^2}^{x_{10}^2 z'/z'} \frac{dx_{21}^2}{x_{21}^2} S_{01}(z') A_{21}(z'). \quad (20)
\end{aligned}$$

It is depicted in the last line of Fig. 3.

Note that Eq. (14) for the neighbor dipole amplitude also has to be modified yielding

$$\begin{aligned}
\Gamma_{02,21}(z') &= \Gamma_{02,21}^{(0)}(z') + \frac{\alpha_s N_c}{2\pi} \int_{z_i}^{z'} \frac{dz''}{z''} \int_{\rho''^2}^{\min\{x_{02}^2, x_{21}^2 z'/z''\}} \frac{dx_{32}^2}{x_{32}^2} \\
&\times [2 \Gamma_{03,32}(z'') S_{23}(z'') + 2 G_{32}(z'') S_{03}(z'') \\
&+ G_{23}(z'') S_{03}(z'') - \Gamma_{02,32}(z'')] \\
&- \frac{\alpha_s N_f}{4\pi} \int_{z_i}^{z'} \frac{dz''}{z''} \int_{\rho''^2}^{x_{21}^2 z'/z''} \frac{dx_{32}^2}{x_{32}^2} \bar{\Gamma}_{03,32}(z''). \quad (21)
\end{aligned}$$

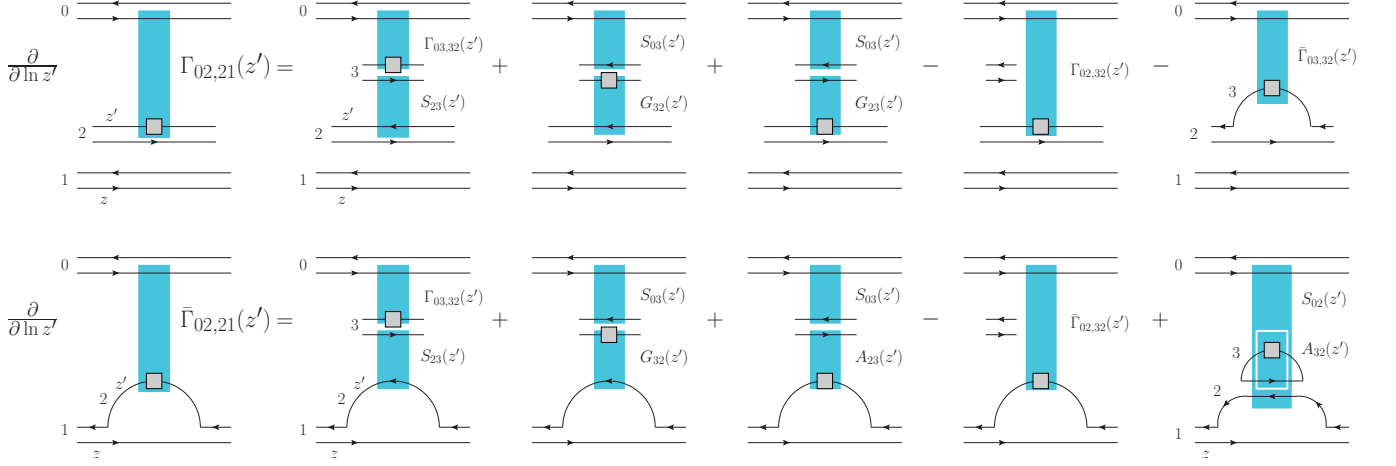


FIG. 4. Large- N_c & N_f helicity evolution for the polarized neighbor dipole amplitudes Γ and $\bar{\Gamma}$.

We also need an equation for $\bar{\Gamma}$:

$$\begin{aligned} \bar{\Gamma}_{02,21}(z') &= \bar{\Gamma}_{02,21}^{(0)}(z') + \frac{\alpha_s N_c}{2\pi} \int_{z_i}^{z'} \frac{dz''}{z''} \int_{\rho'^2}^{\min\{x_{02}^2, x_{21}^2 z'/z''\}} \frac{dx_{32}^2}{x_{32}^2} \\ &\times [\Gamma_{03,32}(z'') S_{23}(z'') + G_{32}(z'') S_{03}(z'') \\ &+ A_{23}(z'') S_{03}(z'') - \bar{\Gamma}_{02,32}(z'')] \\ &+ \frac{\alpha_s N_c}{4\pi} \int_{z_i}^{z'} \frac{dz''}{z''} \int_{\rho'^2}^{x_{21}^2 z'/z''} \frac{dx_{32}^2}{x_{32}^2} S_{02}(z'') A_{32}(z''). \end{aligned} \quad (22)$$

Both of these equations are diagrammatically illustrated in Fig. 4.

Equations (18), (19), (20), (21), and (22) are the large- N_c & N_f helicity evolution equations which are DLA in polarization-dependent terms, but also include LLA saturation corrections through the S -matrices.

In the pure DLA limit we linearize all these equations by putting $S = 1$ in them (we again assume that $G_{01} = G_{10}$, which is true for a large, longitudinally polarized

target):

$$\begin{aligned} Q_{01}(z) &= Q_{01}^{(0)}(z) + \frac{\alpha_s N_c}{2\pi} \int_{z_i}^z \frac{dz'}{z'} \int_{\rho'^2}^{x_{10}^2} \frac{dx_{21}^2}{x_{21}^2} \\ &\times [G_{12}(z') + \Gamma_{02,21}(z') + A_{21}(z') - \bar{\Gamma}_{01,21}(z')] \\ &+ \frac{\alpha_s N_c}{4\pi^2} \int_{z_i}^z \frac{dz'}{z'} \int_{\rho'^2}^{x_{10}^2 z'/z'} \frac{dx_{21}^2}{x_{21}^2} A_{21}(z'), \end{aligned} \quad (23a)$$

$$\begin{aligned} G_{10}(z) &= G_{10}^{(0)}(z) + \frac{\alpha_s N_c}{2\pi} \int_{z_i}^z \frac{dz'}{z'} \int_{\rho'^2}^{x_{10}^2} \frac{dx_{21}^2}{x_{21}^2} \\ &\times [\Gamma_{02,21}(z') + 3G_{12}(z')] \\ &- \frac{\alpha_s N_f}{4\pi} \int_{z_i}^z \frac{dz'}{z'} \int_{\rho'^2}^{x_{10}^2 z'/z'} \frac{dx_{21}^2}{x_{21}^2} \bar{\Gamma}_{02,21}(z'), \end{aligned} \quad (23b)$$

$$\begin{aligned} A_{01}(z) &= A_{01}^{(0)}(z) + \frac{\alpha_s N_c}{2\pi} \int_{z_i}^z \frac{dz'}{z'} \int_{\rho'^2}^{x_{10}^2} \frac{dx_{21}^2}{x_{21}^2} \\ &\times [G_{12}(z') + \Gamma_{02,21}(z') + A_{21}(z') - \bar{\Gamma}_{01,21}(z')] \\ &+ \frac{\alpha_s N_c}{4\pi} \int_{z_i}^z \frac{dz'}{z'} \int_{\rho'^2}^{x_{10}^2 z'/z'} \frac{dx_{21}^2}{x_{21}^2} A_{12}(z'). \end{aligned} \quad (23c)$$

The linearized equations for Γ and $\bar{\Gamma}$ in the large- N_c & N_f

limit become

$$\Gamma_{02,21}(z') = \Gamma_{02,21}^{(0)}(z') + \frac{\alpha_s N_c}{2\pi} \int_{z_i}^{z'} \frac{dz''}{z''} \quad (24a)$$

$$\times \int_{\rho'^2}^{\min\{x_{02}^2, x_{21}^2 z'/z''\}} \frac{dx_{32}^2}{x_{32}^2} [\Gamma_{03,32}(z'') + 3G_{23}(z'')] \\ - \frac{\alpha_s N_f}{4\pi} \int_{z_i}^{z'} \frac{dz''}{z''} \int_{\rho'^2}^{x_{21}^2 z'/z''} \frac{dx_{32}^2}{x_{32}^2} \bar{\Gamma}_{03,32}(z''),$$

$$\bar{\Gamma}_{02,21}(z') = \bar{\Gamma}_{02,21}^{(0)}(z') + \frac{\alpha_s N_c}{2\pi} \int_{z_i}^{z'} \frac{dz''}{z''} \quad (24b)$$

$$\times \int_{\rho'^2}^{\min\{x_{02}^2, x_{21}^2 z'/z''\}} \frac{dx_{32}^2}{x_{32}^2} [\Gamma_{03,32}(z'') + G_{23}(z'') + A_{23}(z'') \\ - \bar{\Gamma}_{02,32}(z'')] + \frac{\alpha_s N_c}{4\pi} \int_{z_i}^{z'} \frac{dz''}{z''} \int_{\rho'^2}^{x_{21}^2 z'/z''} \frac{dx_{32}^2}{x_{32}^2} A_{32}(z''). \quad (24c)$$

Note that in the large- N_c & N_f limit Eqs. (3), (9) and (10) should contain $Q_{10}(z)$ instead of $G_{10}(z)$.

Clearly in the large- N_c / fixed- N_f limit the linearized equations for $G_{01}(z)$ and $\Gamma_{02,21}(z')$ become a closed system of equations (15) again, as employed in the previous Subsection. Since our final observable, quark helicity TMD or hPDF, is related to Q , for the large- N_c limit to be relevant, G should dominate (or at least be comparable to) A .

The linearized equations (23) and (24), when solved, should yield the helicity evolution intercept in the large- N_c & N_f limit. Solution of Eqs. (23) and (24) is left for the future (probably numerical) work.

V. SOLUTION OF THE LARGE- N_c HELICITY EVOLUTION EQUATIONS

Let us now solve Eqs. (15). We start by defining new coordinates,

$$\eta \equiv \ln \frac{z}{z_i}, \quad \eta' \equiv \ln \frac{z'}{z_i}, \quad \eta'' \equiv \ln \frac{z''}{z_i}, \quad (25)$$

$$s_{10} \equiv \ln \frac{1}{x_{10}^2 \Lambda^2}, \quad s_{21} \equiv \ln \frac{1}{x_{21}^2 \Lambda^2}, \quad s_{32} \equiv \ln \frac{1}{x_{32}^2 \Lambda^2},$$

as well as rescaling all η 's and s_{ij} 's,

$$\eta \rightarrow \sqrt{\frac{2\pi}{\alpha_s N_c}} \eta, \quad s_{ij} \rightarrow \sqrt{\frac{2\pi}{\alpha_s N_c}} s_{ij}. \quad (26)$$

Using these variables, we write the large- N_c helicity evolution equations (15) as

$$G(s_{10}, \eta) = G^{(0)}(s_{10}, \eta) + \int_{s_{10}}^{\eta} d\eta' \int_{s_{10}}^{\eta'} ds_{21} \quad (27a)$$

$$\times [\Gamma(s_{10}, s_{21}, \eta') + 3G(s_{21}, \eta')]$$

$$\Gamma(s_{10}, s_{21}, \eta') = \Gamma^{(0)}(s_{10}, s_{21}, \eta') + \int_{s_{10}}^{\eta'} d\eta'' \quad (27b)$$

$$\times \int_{\max\{s_{10}, s_{21} + \eta'' - \eta'\}}^{\eta''} ds_{32} [\Gamma(s_{10}, s_{32}, \eta'') + 3G(s_{32}, \eta'')].$$

Note that the ranges of the s_{21} and s_{32} integrations are restricted to positive values of s_{21} and s_{32} as long as s_{10} is positive; therefore, we always stay above the IR cutoff Λ (in momentum space). The initial conditions for Eqs. (27) are [3]

$$G^{(0)}(s_{10}, \eta) = \Gamma^{(0)}(s_{10}, s_{21}, \eta) \\ = \alpha_s^2 \pi \frac{C_F}{N_c} [C_F \eta - 2(\eta - s_{10})], \quad (28)$$

with $C_F = (N_c^2 - 1)/(2N_c)$. Since the equations at hand are linear, and we are mainly interested in the high-energy intercept, we can scale out $\alpha_s^2 \pi C_F/N_c$.

In order to solve Eqs. (27), we first write down a discretized version of them

$$G_{ij} = G_{ij}^{(0)} + \Delta\eta \Delta s \sum_{j'=i}^{j-1} \sum_{i'=i}^{j'} [\Gamma_{ii'j'} + 3G_{i'j'}], \quad (29a)$$

$$\Gamma_{ijk} = \Gamma_{ijk}^{(0)} + \Delta\eta \Delta s \sum_{j'=i}^{j-1} \sum_{i'=\max\{i, k+j'-j\}}^{j'} [\Gamma_{ii'j'} + 3G_{i'j'}], \quad (29b)$$

where $G_{ij} \equiv G(s_i, \eta_j)$, $\Gamma_{ijk} \equiv \Gamma(s_i, s_k, \eta_j)$, and

$$\Delta\eta = \frac{\eta_{max}}{N_\eta}, \quad \Delta s = \frac{s_{max}}{N_s}, \quad (30)$$

with η_{max} the maximum η value and N_η the number of grid steps in the η direction, and likewise for s_{max} , N_s . The discretized equations (29) are exact in the limit $\Delta\eta, \Delta s \rightarrow 0$ and $\eta_{max}, s_{max} \rightarrow \infty$. To optimize the numerics, we set $\eta_{max} = s_{max}$.

With the discretized evolution equations (29) in hand (along with the initial conditions (28) suitably discretized), we first choose values for $\eta_{max} = s_{max}$ and $\Delta\eta = \Delta s$. We then systematically go through the η - s grid in such a way that each G_{ij} (and Γ_{ijk}) only depends on G, Γ values that have already been calculated. Thus, we can determine G_{ij} for each i, j . Our numerical solution (for $\eta_{max} = 40$, $\Delta\eta = 0.05$) is plotted in Fig. 5.

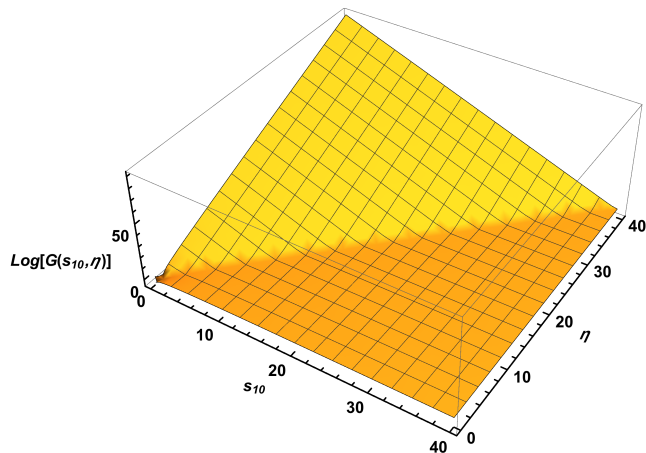


FIG. 5. The numerical solution of Eqs. (27) for the polarized dipole amplitude G plotted as a function of rescaled “rapidity” η and transverse variable s_{10} .

We find

$$\Delta q^S(x, Q^2) \sim \Delta \Sigma(x, Q^2) \sim \left(\frac{1}{x}\right)^{\alpha_h} \quad (31)$$

with

$$\alpha_h = 2.31 \sqrt{\frac{\alpha_s N_c}{2\pi}}, \quad (32)$$

where we have reinstated the factor $\sqrt{\alpha_s N_c / 2\pi}$ originally scaled out by Eq. (26).

We note that the value in Eq. (32) is in disagreement with the “pure glue” intercept of $3.66\sqrt{\alpha_s N_c / 2\pi}$ obtained by BER [6] by about 35%. In [3] we identify DLA diagram contributions not included by the authors of [6] in their treatment of the problem. We believe that omitting those diagrams limited the resummation of [6] to the leading-twist contribution only. In comparison, our result (32) resums all twists at small x .

Interestingly, the leading twist approximation to $\alpha_P - 1$ in BFKL evolution is larger than the exact all-twist intercept by about 30% [7]; it is possible that something similar is occurring for helicity evolution. In Ref. [3], we have explored this possibility, performed various analytical cross-checks of our helicity evolution equations, and compared to BER where possible; we have not found any inconsistencies in our result.

VI. IMPACT ON THE PROTON SPIN

In order to determine the quark and gluon spin based on Eq. (1), one needs to extract the helicity PDFs. There are several groups who have performed such analyses, e.g., DSSV [8, 9], JAM [10, 11], LSS [12–14], NNPDF [15, 16]. While the focus at small x has been on the behavior of $\Delta G(x, Q^2)$, there is actually quite a bit of uncertainty in the size of $\Delta \Sigma(x, Q^2)$ in that regime as well.

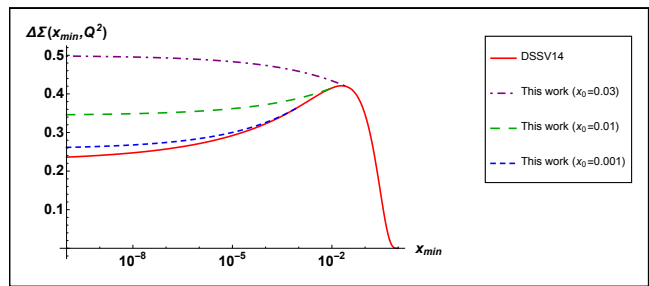


FIG. 6. Plot of $\Delta \Sigma^{[x_{min}]}(Q^2)$ vs. x_{min} at $Q^2 = 10 \text{ GeV}^2$. The solid curve is from DSSV14 [9]. The dot-dashed, long-dashed, and short-dashed curves are from various small- x modifications of $\Delta \Sigma(x, Q^2)$ at $x_0 = 0.03, 0.01, 0.001$, respectively, using our helicity intercept (see the text for details).

Let us define the truncated integral

$$\Delta \Sigma^{[x_{min}]}(Q^2) \equiv \int_{x_{min}}^1 dx \Delta \Sigma(x, Q^2). \quad (33)$$

One finds for DSSV14 [9] that the central value of the full integral $\Delta \Sigma^{[0]}(10 \text{ GeV}^2)$ is about 40% smaller than $\Delta \Sigma^{[0.001]}(10 \text{ GeV}^2)$. The NNPDF14 [16] helicity PDFs lead to a similar decrease, although, due to the nature of neural network fits, the uncertainty in this extrapolation is 100%. On the other hand, for JAM16 [11] helicity PDFs the decrease from the truncated to the full integral of $\Delta \Sigma(x, Q^2)$ seems to be at most a few percent. The origin of this uncertainty, and more generally the behavior of $\Delta \Sigma(x, Q^2)$ at small x , is mainly due to varying predictions for the size and shape of the sea helicity PDFs, in particular $\Delta s(x, Q^2)$ [8–11, 15–17]. So far, the only constraint on $\Delta s(x, Q^2)$, and how it evolves at small x , comes from the weak neutron and hyperon decay constants. Therefore, there is a definite need for direct input from theory on the small- x intercept of $\Delta \Sigma(x, Q^2)$: this is what we have provided in this Letter.

We now will attempt to quantify how the small- x behavior of $\Delta \Sigma(x, Q^2)$ derived here affects the integral in Eq. (1). We take a simple approach and leave a more rigorous phenomenological study for future work. First, we attach a curve $\Delta \tilde{\Sigma}(x, Q^2) = N x^{-\alpha_h}$ (with α_h given in (32)) to the DSSV14 result for $\Delta \Sigma(x, Q^2)$ at a particular small- x point x_0 . Next, we fix the normalization N by requiring $\Delta \tilde{\Sigma}(x_0, Q^2) = \Delta \Sigma(x_0, Q^2)$. Finally, we calculate the truncated integral (33) of the modified quark helicity PDF

$$\Delta \Sigma_{mod}(x, Q^2) \equiv \theta(x - x_0) \Delta \Sigma(x, Q^2) + \theta(x_0 - x) \Delta \tilde{\Sigma}(x, Q^2) \quad (34)$$

for different x_0 values. The results are shown in Fig. 6 for $Q^2 = 10 \text{ GeV}^2$ and $\alpha_s \approx 0.25$, in which case $\alpha_h \approx 0.80$.

We see that the small- x evolution of $\Delta \Sigma(x, Q^2)$ could offer a moderate to significant enhancement to the quark spin, depending on where in x the effects set in and on the parameterization of the helicity PDFs at higher x .

Thus, it will be important to incorporate the results of this work, and more generally the small- x helicity evolution equations discussed here, into future extractions of helicity PDFs.

VII. SUMMARY

In [1, 3] we have derived small- x evolution equations for the polarized dipole amplitude. The equations close in the large- N_c and large- N_c & N_f limits. The large- N_c equations are presented above. The solution of these equations provides theoretical input on the perturbative value of the small- x intercept for the quark helicity TMD and PDF, and for the g_1 structure function.

We have also numerically solved the small- x helicity evolution equations (15) of Ref. [1] in the large- N_c limit. We found an intercept of $\alpha_h = 2.31\sqrt{\alpha_s N_c/2\pi}$, which, from Eq. (31), is a direct input from theory on the behavior of $\Delta\Sigma(x, Q^2)$ at small x . Although a more rigorous

phenomenological study is needed, we demonstrated in a simple approach that such an intercept could offer a moderate to significant enhancement of the quark contribution to the proton spin. Therefore, it appears imperative to include the effects of the small- x helicity evolution discussed here in future fits of helicity PDFs, especially those to be obtained at an Electron-Ion Collider.

ACKNOWLEDGMENTS

This material is based upon work supported by the U.S. Department of Energy, Office of Science, Office of Nuclear Physics under Award Number DE-SC0004286 (YK) and within the framework of the TMD Topical Collaboration (DP) and DOE Contract No. DE-SC0012704 (MS). MS received additional support from an EIC program development fund from BNL and from the U.S. Department of Energy, Office of Science under the DOE Early Career Program.

-
- [1] Y. V. Kovchegov, D. Pitonyak, and M. D. Sievert, *JHEP* **01**, 072 (2016), arXiv:1511.06737 [hep-ph].
 - [2] Y. V. Kovchegov, D. Pitonyak, and M. D. Sievert, (2016), arXiv:1610.06188 [hep-ph].
 - [3] Y. V. Kovchegov, D. Pitonyak, and M. D. Sievert, (2016), arXiv:1610.06197 [hep-ph].
 - [4] Y. V. Kovchegov and M. D. Sievert, *Nucl. Phys.* **B903**, 164 (2016), arXiv:1505.01176 [hep-ph].
 - [5] K. Itakura, Y. V. Kovchegov, L. McLerran, and D. Teaney, *Nucl. Phys.* **A730**, 160 (2004), arXiv:hep-ph/0305332.
 - [6] J. Bartels, B. Ermolaev, and M. Ryskin, *Z.Phys.* **C72**, 627 (1996), arXiv:hep-ph/9603204 [hep-ph].
 - [7] Y. V. Kovchegov and E. Levin, *Quantum Chromodynamics at High Energy* (Cambridge University Press, 2012).
 - [8] D. de Florian, R. Sassot, M. Stratmann, and W. Vogelsang, *Phys. Rev.* **D80**, 034030 (2009), arXiv:0904.3821 [hep-ph].
 - [9] D. de Florian, R. Sassot, M. Stratmann, and W. Vogelsang, *Phys. Rev. Lett.* **113**, 012001 (2014), arXiv:1404.4293 [hep-ph].
 - [10] P. Jimenez-Delgado, A. Accardi, and W. Melnitchouk, *Phys. Rev.* **D89**, 034025 (2014), arXiv:1310.3734 [hep-ph].
 - [11] N. Sato, W. Melnitchouk, S. E. Kuhn, J. J. Ethier, and A. Accardi (Jefferson Lab Angular Momentum), *Phys. Rev.* **D93**, 074005 (2016), arXiv:1601.07782 [hep-ph].
 - [12] E. Leader, A. V. Sidorov, and D. B. Stamenov, *Phys. Rev.* **D73**, 034023 (2006), arXiv:hep-ph/0512114 [hep-ph].
 - [13] E. Leader, A. V. Sidorov, and D. B. Stamenov, *Phys. Rev.* **D82**, 114018 (2010), arXiv:1010.0574 [hep-ph].
 - [14] E. Leader, A. V. Sidorov, and D. B. Stamenov, *Phys. Rev.* **D91**, 054017 (2015), arXiv:1410.1657 [hep-ph].
 - [15] R. D. Ball, S. Forte, A. Guffanti, E. R. Nocera, G. Ridolfi, and J. Rojo (NNPDF), *Nucl. Phys.* **B874**, 36 (2013), arXiv:1303.7236 [hep-ph].
 - [16] E. R. Nocera, R. D. Ball, S. Forte, G. Ridolfi, and J. Rojo (NNPDF), *Nucl. Phys.* **B887**, 276 (2014), arXiv:1406.5539 [hep-ph].
 - [17] E. C. Aschenauer, R. Sassot, and M. Stratmann, *Phys. Rev.* **D92**, 094030 (2015), arXiv:1509.06489 [hep-ph].